JOURNAL OF SPACECRAFT AND ROCKETS
Vol. 39, No. 5, September–October 2002

Corner Wrinkling of a Square Membrane Due to Symmetric Mechanical Loads

Joseph R. Blandino*
James Madison University, Harrisonburg, Virginia 22807
John D. Johnston†
NASA Goddard Spaceflight Center, Greenbelt, Maryland 20771
and
Urmil K. Dharamsi‡
James Madison University, Harrisonburg, Virginia 22807

Thin-film membrane structures are under consideration for use in many future gossamer spacecraft systems. Examples include sunshields for large-aperture telescopes, solar sails, and membrane optics. The development of capabilities for testing and analyzing pretensioned, thin-film membrane structures is an important and challenging aspect of gossamer spacecraft technology development. Results are presented from experimental and computational studies performed to characterize the wrinkling behavior of thin-film membranes under mechanical loading. The test article is a 500-mm-square Kapton® membrane subjected to symmetric corner loads. Data are presented for loads ranging from 0.49 to 4.91 N. The experimental results show that as the load increases the number of wrinkles increases, while the wrinkle amplitude decreases. The computational model uses a finite element implementation of Stein–Hedgepeth membrane wrinkling theory to predict the behavior of the membrane. Comparisons were made with experimental results for the wrinkle angle and wrinkled region. There was reasonably good agreement between the measured wrinkle angle and the predicted directions of the major principle stresses. The shape of the wrinkled region predicted by the finite element model matches that observed in the experiments; however, the size of the predicted region is smaller that that determined in the experiments.

Nomenclature

d	=	distance along diagonal cut
E	=	modulus of elasticity
K_{slack}	=	stiffness matrix for slack elements
K_{taut}	=	stiffness matrix for taut elements
K_{wrinkled}	=	stiffness matrix for wrinkled elements
L	=	length of diagonal cut
P	=	applied load
X, Y, Z	=	coordinates
α	=	principle stress angle
ν	=	Poisson's ratio

Introduction

VERY large, ultralightweight or gossamer spacecraft are an enabling technology for many future space missions. Thin-film membrane structures (including sunshields, solar sails, inflatable antennas, and membrane optics) are a common element in these systems. Because of to their unprecedented size and flexibility, gossamer spacecraft systems will require advanced modeling and testing technologies to support their development. The behavior of these structures can be highly nonlinear and challenging to model and test. Modeling and analysis techniques to predict nonlinear membrane behavior such as wrinkling should be validated through comparison with test results. However, ground testing of ultralightweight structures is inherently difficult due to the presence of gravity and the influence of instrumentation mass on structural behavior, and new test methods and noncontact instrumentation are needed. These needs are specifically addressed through the study of analytical and experimental capabilities to predict the wrinkling behavior of a simple thin-film membrane structure.

Received 13 July 2001; revision received 28 May 2002; accepted for publication 28 May 2002.

*Assistant Professor, Integrated Science and Technology Program, MSC 4102; blandijx@jmu.edu. Member AIAA.
†Aerospace Engineer, Mechanical Systems Analysis and Simulation Branch, Code 542, Next Generation Space Telescope Mechanical Systems Team; John.D.Johnston.1@gsfc.nasa.gov. Member AIAA.
‡Undergraduate Research Assistant, Integrated Science and Technology Program, MSC 4102; dharamuk@jmu.edu.

Previous Studies

When a thin-film membrane is subjected to discrete tensile preloads, localized buckling (or wrinkling) often results. Wrinkles form because thin membranes have negligible bending stiffness and cannot resist compressive loads.[1] The wrinkles serve to eliminate compressive stresses. The behavior of membrane structures has been studied previously by numerous researchers. A comprehensive overview of the modeling and analysis of membranes completed by Jenkins and Leonard discusses many important contributions to this field of research.[2] Finite element modeling techniques will be utilized extensively to predict the behavior of future thin-film membrane structures due to the nonlinear nature of the problem. Typically, the capabilities of commercially available finite element codes are inadequate to model all of the important aspects of membrane behavior. For example, modeling thin-film membrane structures using standard membrane elements is not advisable when the membranes experience significant wrinkling because the stress distribution in the membranes will not be represented properly. There are several approaches available for modeling membrane structures that account for the effects of wrinkles, including the cable network method and modified membrane element methods.[3] The cable network method was developed specifically for modeling the dynamics of pretensioned, wrinkled membranes. The approach is based on the established principle that load transfer in wrinkled regions takes place along wrinkle lines. The membrane is meshed with a network of cables (preloaded bar elements) that is mapped to the wrinkle pattern of the structure. This approach is useful for determining the out-of-plane structural dynamic characteristics of pretensioned, wrinkled membrane structures; however, the method is limited in that it requires prior knowledge of the wrinkle pattern to create the cable network and does not account for in-plane shear or thermal effects. The cable network method has been previously used

to model the inflatable sunshield in space and $\frac{1}{10}$th scale model Next Generation Space Telescope (NGST) sunshield.[4,5] A more accurate representation of wrinkled membrane structural behavior can be obtained by using standard membrane finite elements in conjunction with a no-compression membrane material model.[3,6,7] These approaches start by developing a set of criteria by which the state of the membrane (wrinkled, slack, or taut) can be assessed. During the analysis, the material properties of each element are adjusted to account for the behavior associated with the particular state of that element. The advantages of these methods are that they can be used to 1) determine accurately the state of stress in the membrane in the presence of wrinkling, 2) predict wrinkle characteristics including wrinkled region geometry and wrinkle directions, and 3) model thermal–structural behavior.

Relatively few experimental studies concerning the behavior of pretensioned, thin-film membranes for space structures applications have been carried out over the years. During the 1980s, a small amount of attention was given to membranes that would serve as reflector facets attached to a stiff underlying structure. Reports by Sewall et al.[8] at the NASA Langley Research Center and Thomas and Veal at the Air Force Rocket Propulsion Laboratory[9] are notable for this era on the subject of thin-film tensioned membranes. The analysis and testing of inflatable structures, that is, tubes and antennas, received considerable attention in the 1990s. Of particular relevance to this research are those studies involving pretensioned flat membrane structures, that is, solar sails, sunshields, and optical membrane flats. Jenkins,[10] Wong,[7] and Kukathasan[11] have published results in the past few years examining both the static and/or dynamic response of pretensioned thin-film membrane structures including experimental studies. Testing of membranes is inherently difficult not only because of the presence of gravity, but also because any instrumentation contacting the surface will alter membrane behavior. Two techniques have been employed successfully in the past to measure the surface of membrane structures. Jenkins et al.[10] used a capacitance-based proximity sensor to measure the surface wrinkling of an isothermal membrane subjected to combined shear and tension loads. The sensor operated by measuring the change in capacitance between the sensor head and the membrane surface. This technique resolved out-of-plane wrinkle amplitudes as small as ± 0.05 mm. Recently, Pappa et al. employed photogrammetry to determine the surface figure of a 5.0-m-diam inflatable space antenna.[12] Photogrammetry is a technique that is commonly used by geographers and cartographers. It is the science of constructing a three-dimensional contour map by triangulating common points from a series of two-dimensional images. On a relatively large structure this technique had a precision on the out-of-plane displacements of between 0.9 and 2.8 mm. These were obtained with a digital camera that had a resolution of 1792×1200 pixels. Both a capacitance sensor and photogrammetry were used by Blandino et al.[13] to study the behavior of a square membrane subjected to both mechanical and thermal loads.

This paper presents an experimental investigation into the wrinkling of a square Kapton® membrane that is subjected to symmetric mechanical loads at the corners, and a comparison of those results with predictions from a finite element model. The goal of the research is to quantify the wrinkle patterns near a membrane corner over a range of mechanical loads. The knowledge gained from this study will provide valuable insight into the phenomenon of membrane wrinkling. The data will also be useful for validating current modeling techniques.

Experiment Design

The design of the experiments is described in this section, including the test specimen, test frame, load cases, and instrumentation.

Test Specimen

The test specimen used for this study was a 0.5 m square Kapton HN membrane 2.54×10^{-2} mm thick. The membrane has a 1×10^{-3} mm vapor deposited aluminum coating on one side. The test article was cut from a roll of material and was free of creases. The corners were reinforced with 0.12-mm-thick transparency film on both sides. The reinforcing was triangular in shape with dimensions of approximately $10.0 \times 10.0 \times 14.1$ mm. Mechanical loads were applied at discrete points at the corners of the membrane via Kevlar® threads. Kevlar threads were also used to anchor the corners opposite the loads to the test frame.

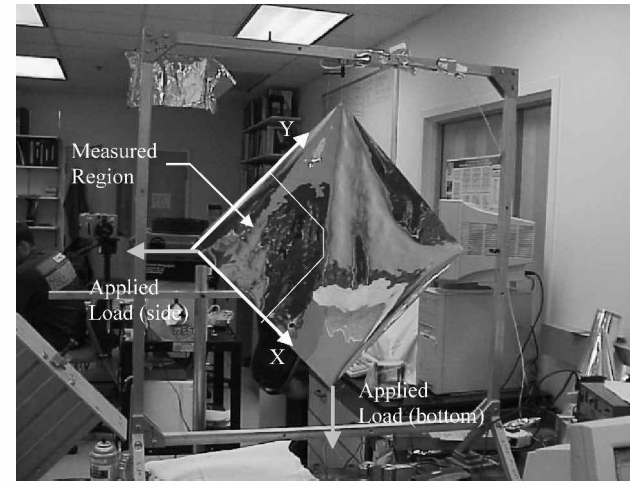

Fig. 1 Membrane mounted in test frame; axes, direction of applied loads, and measured region.

Test Frame

The membrane was oriented in the test frame and the axes taken as shown in Fig. 1. The frame was constructed from 25.4-mm, 6061 aluminum square stock. The frame was 980×980 mm. The corners of the frame were reinforced with 6.35-mm aluminum plates. These aided in squaring the frame during assembly. Two legs were mounted to the frame at each of the bottom corners. Each leg met the frame at a 45-deg angle. The legs were fabricated from aluminum stock identical to that used for the frame. The legs rested on vibration isolation pads. The thread attached to the top corner of the membrane was run through a 0.41-mm-diam hole in a Delrin® plug. The plug was attached to a mounting screw on the test frame. The thread on the right corner was attached to a mounting screw in an identical manner. The threads attached to the bottom and left sides were passed through 0.41-mm-diam holes in Delrin plugs mounted to the test frame. Mechanical loads were applied by hanging masses from the ends of these threads. Once the membrane was loaded, the Kevlar threads were checked to ensure that they were square with the test frame. Excess thread at the top and right side were pulled taut and securely fastened to the test frame so that the membrane could not slip. During the squaring procedure and testing, both axes were loaded symmetrically. Before hanging, the manufacturer's value for each mass was verified using an electronic balance.

Load Cases

A single membrane was used for a test series of four load cases. This allowed direct comparison between wrinkle patterns from case to case. The test sequence began with approximately a 0.49-N load applied as discussed earlier. The mass remained unchanged for approximately 15 min while measurements of the membrane were taken. At the completion of a test case, additional mass was added to the two corners and the sequence started again until the four load cases were completed. The desired loads and the actual loads applied to the corners are shown in Table 1.

Instrumentation

Photogrammetry was used to measure the surface profile within a pentagon-shaped section that was approximately $250.0 \times 250.0 \times 212.5 \times 212.5 \times 53.0$ mm in size with the apex located at the left corner of the membrane. The location of the measured area is shown in Fig. 1. A symmetric pattern of spots was projected onto the nonaluminized side of the membrane using a standard slide projector and 35-mm slide. The projected spots were approximately 3.1 mm on

Table 1 Summary of applied loads

Case	Desired load, N	Actual loads, N	
		Side	Bottom
1	0.491	0.490	0.483
2	1.471	1.470	1.462
3	2.452	2.450	2.442
4	4.905	4.898	4.891

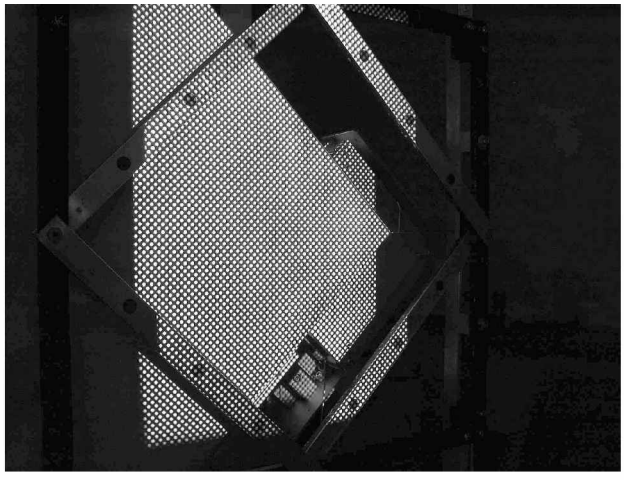

a) Left image used for photogrammetry

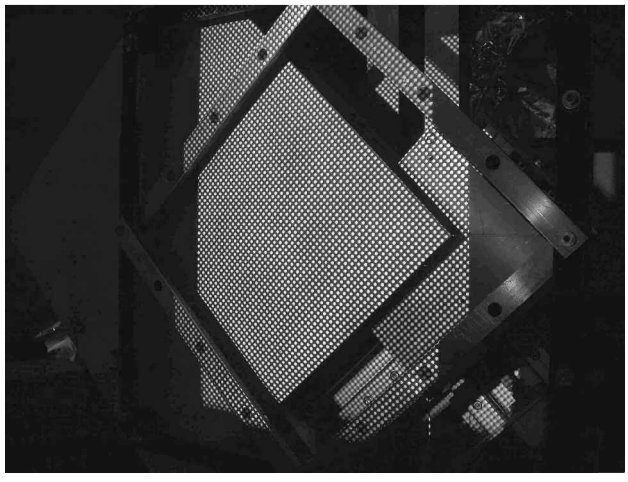

b) Right image used for photogrammetry

Fig. 2 Typical images used for photogrammetry; note frame with control points.

center and 3.1 mm in diameter. To determine the spatial coordinates accurately, the center of each target spot must be located in each image. Locating the center of each target can be done automatically by the photogrammetry software used, provided that the spots are uniformly illuminated. Even the nonaluminized side of the membrane produced glare and nonuniform contrast across the membrane; therefore, this side of the membrane was sprayed with a talc-based developer. This type of developer is typically used to locate surface cracks in materials. The solution dried white and adhered but did not bond to the membrane surface. It could be wiped off easily. The coating provided a nonreflective surface to project targets onto the membrane. Two images were taken with identical, calibrated, digital cameras mounted approximately 610 mm from the membrane surface. The baseline between the two cameras was approximately 580 mm. The cameras had a 2048 × 1536 pixel resolution. The images were processed using ShapeCapture, a commercially available photogrammetry software package designed for use with digital images. Photographs of the membrane with dot pattern are shown in Figs. 2a and 2b.

A frame with control points surrounded the test area. The frame can be seen in Figs. 2a and 2b. The frame was square with side lengths of 381 mm constructed from 25.4 mm wide × 6.25 mm thick aluminum. Each side had three equally spaced control points. The control points were 12.5 mm in diameter, machined 0.254 mm below the surface of the aluminum, and painted black. The control points were used to define the axes and determine image scale. This information was used within the software during the analysis and was also used to determine the accuracy of the measurements. Typical errors for X, Y, and Z measurements were estimated by the photogrammetry software to be approximately 1.25×10^{-3}, 1.25×10^{-3}, and 2.25×10^{-3} mm, respectively.

Although the images used for photogrammetry are of the nonaluminized side of the membrane, the results presented are for the aluminized face of the membrane, that is, facing the aluminized side of the membrane at the left corner shown in Fig. 1. The photogrammetry software outputs columns of X, Y, and Z coordinates. For the section of membrane under study, coordinates for approximately 2000 data points were collected. The data were put into matrix form using the kriging method available within the Surfer Version 7 plotting software. Once the data were in matrix form, a smoothing operation is performed and the results plotted.

Note that the amplitude data near the edge of the membrane may not always be reliable. Near the edges, the radius of curvature of the membrane can be relatively small. This caused problems focusing targets and presumably errors in the stereo matching between points. This type of error can result in incorrect determination of the amplitude value for the data point. Therefore, data points near the membrane edges that had Z values significantly different from adjacent points were judiciously removed before processing the data.

Experimental Results

The main goal of this investigation was to quantify the wrinkle pattern near the corner of a symmetrically loaded membrane. Experimental data were collected that determined the effect of loading on the number of wrinkles, wrinkle amplitude, and wrinkle angle. In this section results are presented for the four load cases in Table 1.

The first objective was to determine the number of wrinkles present for each load case. Figures 3–6 show contour plots for each case. Cases 1 and 2 have two wrinkles, whereas cases 3 and 4 show four distinct wrinkles. Thus, as the loads increased, the number of wrinkles was observed to increase. These results are in agreement with those reported by Jenkins et al.[10] Their study of a Mylar® membrane subjected to combined tension and shear loads reported that the number of wrinkles increased as the tension load increased. Also note in Figs. 3 and 4 that curling of the membrane edges is

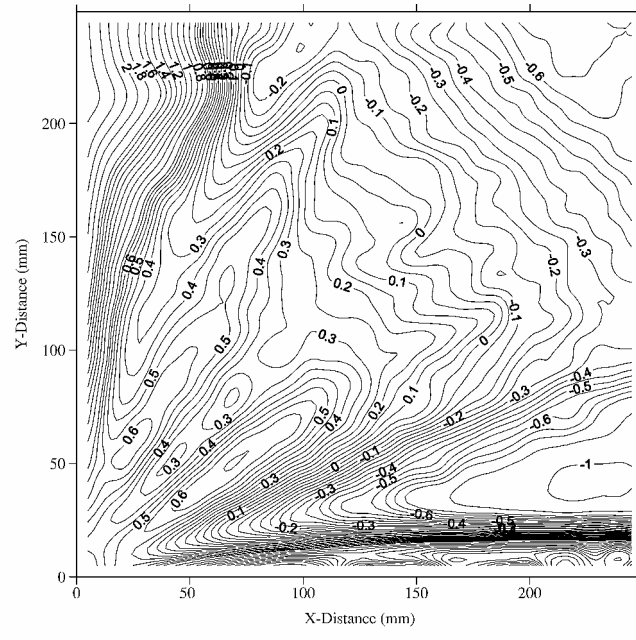

Fig. 3 Contour plot of corner section of membrane subjected to 0.49-N loads.

Table 2 Wrinkle angle measured from *X* axis

	Angle, deg			
Location	0.49 N	1.47 N	2.45 N	4.90 N
Valley 1	62.48	72.26	76.49	80.40
Peak 1	58.88	62.32	71.95	73.52
Valley 2	45.13	49.05	68.08	65.99
Peak 2	36.21	35.04	62.24	58.97
Valley 3	10.75	8.51	46.19	47.15
Peak 3	——	——	37.63	39.57
Valley 4	——	——	27.49	33.40
Peak 4	——	——	25.70	25.74
Valley 5	——	——	9.69	11.74

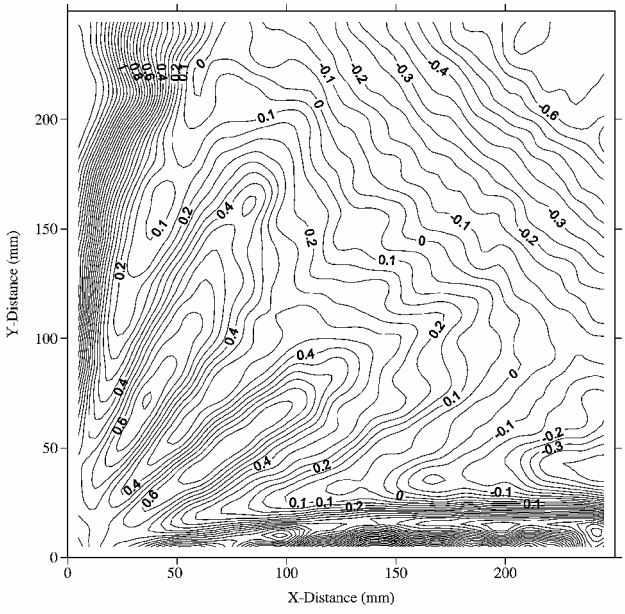

Fig. 4 Contour plot of corner section of membrane subjected to 1.47-N loads.

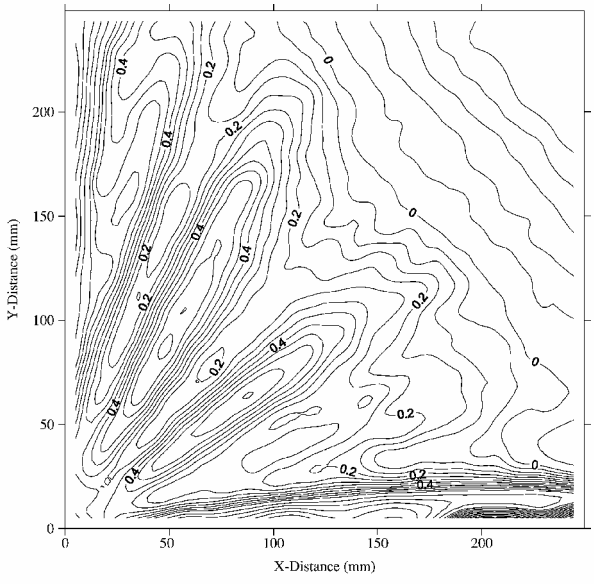

Fig. 5 Contour plot of corner section of membrane subjected to 2.45-N loads.

evident along the *Y* axis. Curling of the edges naturally occurs because there is no loading normal to the free edges of the membrane.

The wrinkle angle was determined by measuring the direction of each wrinkle with respect to the *X* axis. Angle measurement was done using the contour plots. Lines were drawn on the contour plots as shown in Fig. 7. In Fig. 7, valleys are denoted by a V, and peaks are denoted by a P. The angle measurements for all load cases appear in Table 2.

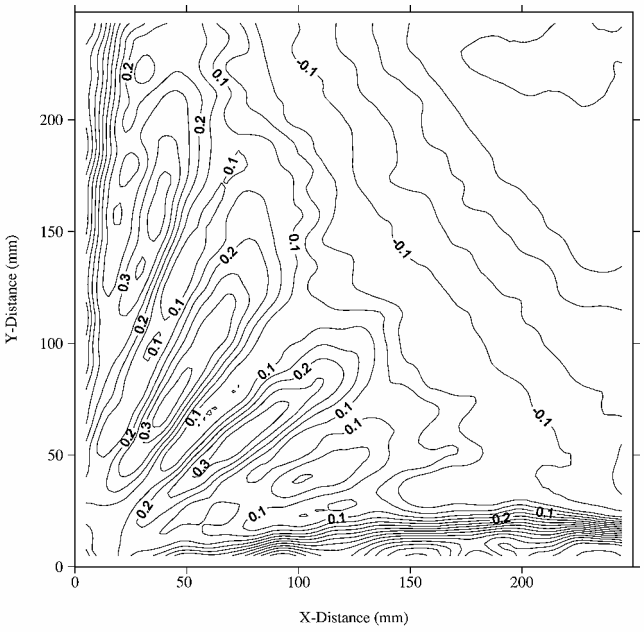

Fig. 6 Contour plot of corner section of membrane subjected to 4.90-N loads.

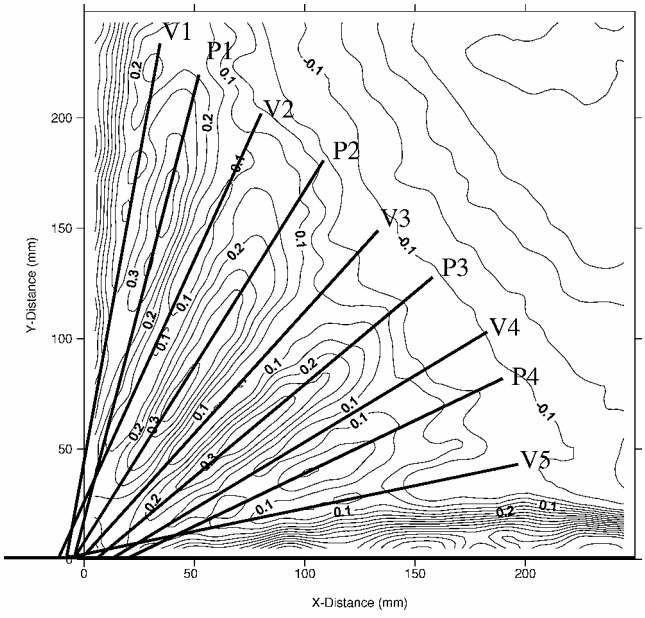

Fig. 7 Typical contour plot showing location of valleys and peaks with respect to the *X* axis.

To measure the wrinkle amplitude, the displacement data along diagonals from $Y = 80$ mm to $X = 80$ mm, $Y = 100$ mm to $X = 100$ mm, and $Y = 150$ mm to $X = 150$ mm were plotted in Figs. 8a–8c. Data along the diagonal were used because it was approximately perpendicular to the wrinkles. Wrinkle amplitude was determined by measuring the difference between the valley near the center of the diagonal to the two nearest peaks. Figures 8 show that, in general, the wrinkle amplitude decreases with increasing load. Figures 8b and 8c show that for the case 1 the wrinkle amplitude is approximately 0.5 mm, whereas for case 4, it is 0.25 mm. These results are also in agreement with those reported by Jenkins et al.[10]

Analysis of Experiments

An analysis of the laboratory experiments was performed to predict the wrinkling behavior of the membrane. The following sections discuss the technique used to analyze the wrinkled membrane, the details of the finite element model, and a summary of the results including a comparison between analytical predictions and experimental results.

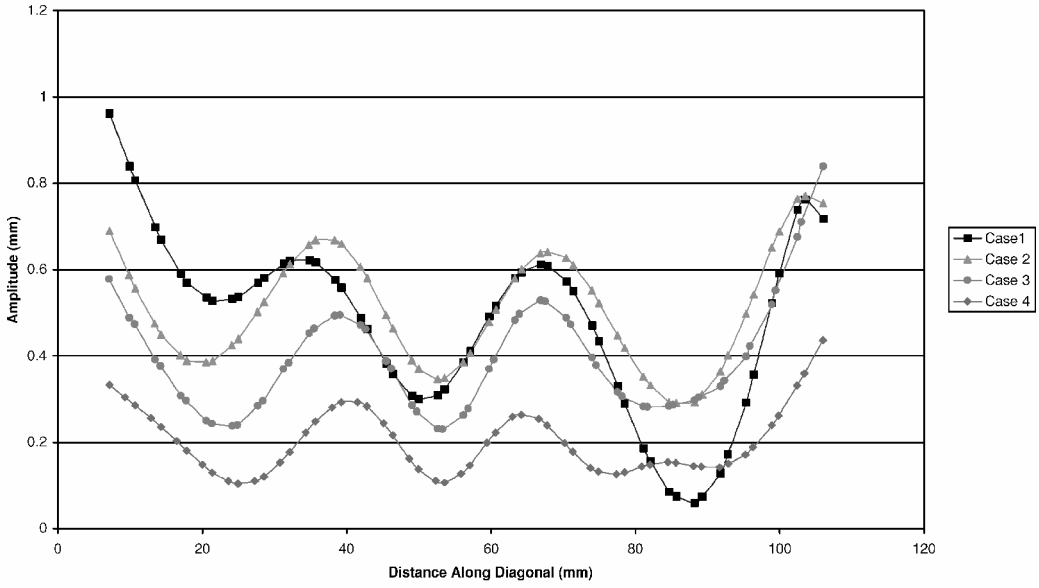

a) $Y = 80$ mm to $X = 80$ mm

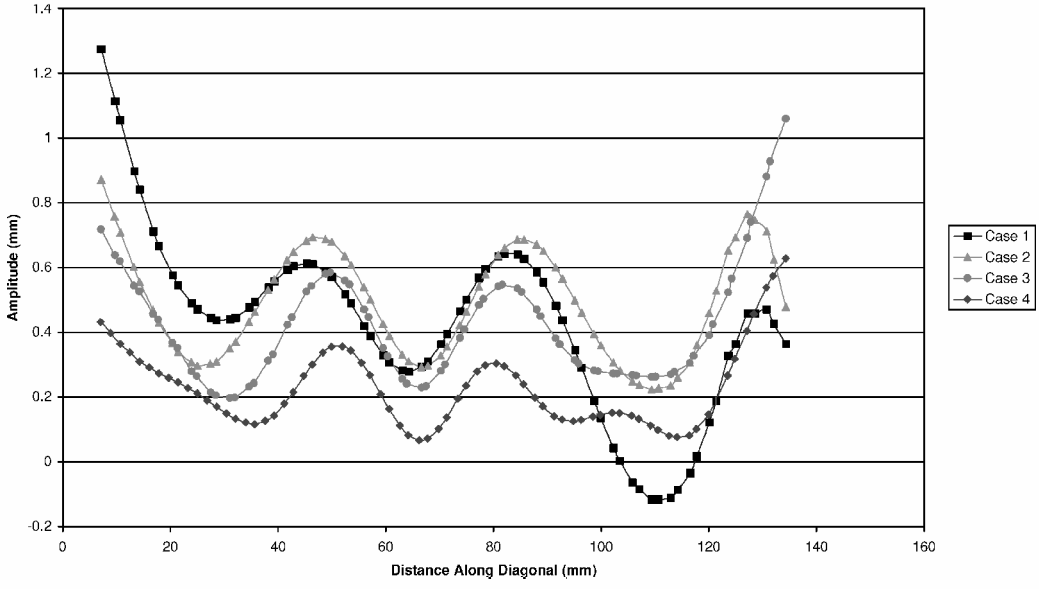

b) $Y = 100$ mm to $X = 100$ mm

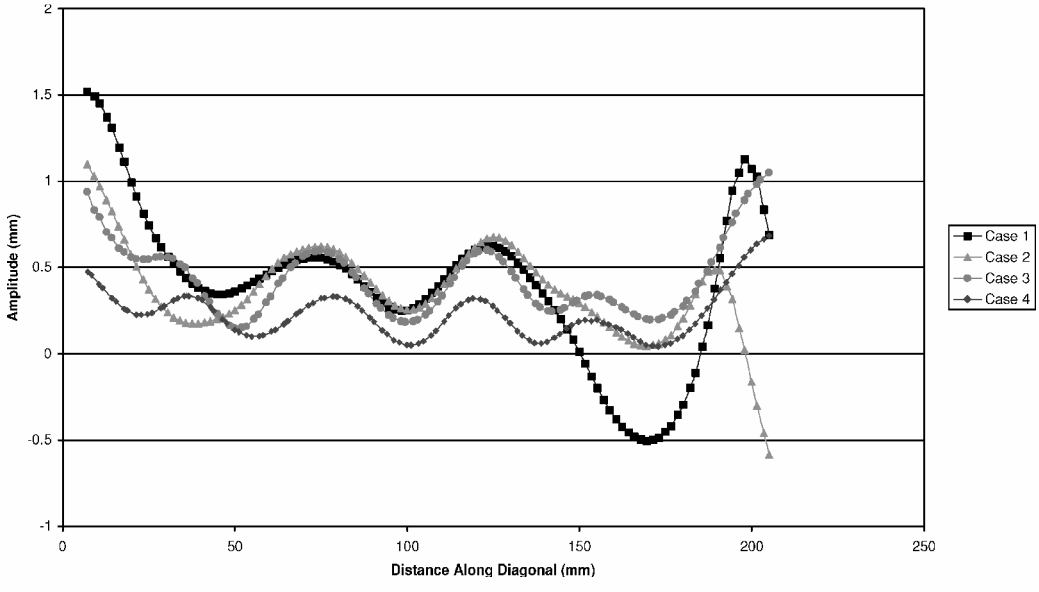

c) $Y = 150$ mm to $X = 150$ mm

Fig. 8 Amplitude data along a diagonal line.

Analysis Technique

Nonlinear analysis techniques are required to account for accurately geometric nonlinearities, load stiffening, and wrinkling effects in the analysis of membrane structures. The present analysis is performed using the commercially available finite element analysis program ABAQUS.[14] A nonlinear static analysis with membrane wrinkling effects accounted for through the use of a user-defined material (UMAT) subroutine is used to predict the structural response of the membrane. The UMAT utilized here was developed by Adler[15] based on work by Miller and Hedgepeth.[16] In this approach, membrane element material properties are iteratively modified during the analysis to account for the effects of wrinkling and slackness. The analysis procedure is as follows. First, a finite element model of the structure is generated using membrane elements that are assigned the wrinkling material model. Next, a nonlinear static analysis of the structure is performed during which the state of each element (taut, slack, or wrinkled) is determined. A combined stress–strain criterion is used in the UMAT to determine the element states. Kang and Im[17] have suggested that the combined stress–strain criterion is superior to a stress-only criterion because it avoids ambiguities between wrinkled and slack states for isotropic materials and offers an advantage over a strain-only criterion in that it is also applicable to anisotropic materials. Following the elements state determination, the stiffness matrix of each element is updated as follows. If the element state is taut, the stiffness matrix is unaltered:

$$K_{\text{taut}} = \frac{E}{(1-\nu^2)} \begin{bmatrix} 1 & \nu & 0 \\ \nu & 1 & 0 \\ 0 & 0 & \dfrac{1-\nu}{2} \end{bmatrix} \tag{1}$$

If the element state is slack, the stiffness matrix is set equal to zero:

$$K_{\text{slack}} = \begin{bmatrix} 0 & 0 & 0 \\ 0 & 0 & 0 \\ 0 & 0 & 0 \end{bmatrix} \tag{2}$$

If the element state is wrinkled, the stiffness matrix is modified according to Stein–Hedgepeth[1] wrinkling theory (see Ref. 16):

$$K_{\text{wrinkled}} = \frac{E}{4} \begin{bmatrix} 2(1+P) & 0 & Q \\ 0 & 2(1-P) & Q \\ Q & Q & 1 \end{bmatrix} \tag{3}$$

where $P = 2\cos(\alpha)$ and $Q = 2\sin(\alpha)$. Stein–Hedgepeth[1] wrinkling theory predicts that the stress state in a wrinkled region of a membrane is uniaxial (positive major principal stress and zero minor principal stress) and that wrinkles form in straight lines along the direction of the major principal stresses. (Load transfer in the wrinkled region is along these lines.) Note that this theory predicts average strains and displacements in the wrinkled region, but not individual wrinkle details. Further details regarding the UMAT developed by Adler can be found in Ref. 15.

Finite Element Model

The finite element model of the laboratory experiment is shown in Fig. 9. The model includes the membrane, corner reinforcements, and Kevlar threads. The membrane is modeled using 39976 membrane elements (ABAQUS M3D4 and M3D3 elements), which are assigned the wrinkling material model. The corners are modeled with 64 shell elements (ABAQUS S3 elements), and the threads are represented using 20 beam elements (ABAQUS B31 elements). A summary of material properties used in the analysis is presented in Table 3. The point loads are applied at the ends of the left and bottom Kevlar threads. The boundary conditions are applied at the ends of the Kevlar threads attached to the test fixture. The ends of the top and right threads are constrained in all three translational degrees of freedom, whereas the left and bottom threads are constrained in the two translational degrees of freedom normal to the loading direction.

Table 3 Summary of material properties

Component	Material	E, N/m^2	ν
Membrane	Kapton HN	2.5E+9	0.34
Corner reinforcement	Mylar	3.8E+9	0.30
Thread	Kevlar	7.1E+10	0.36

Table 4 Summary of predicted membrane stresses

Load case	$\sigma_{\max}$, N/m^2	σ_{center}, N/m^2
1	1.49E+6	4.26E+4
2	4.49E+6	1.28E+5
3	7.50E+6	2.13E+5
4	1.51E+7	4.25E+5

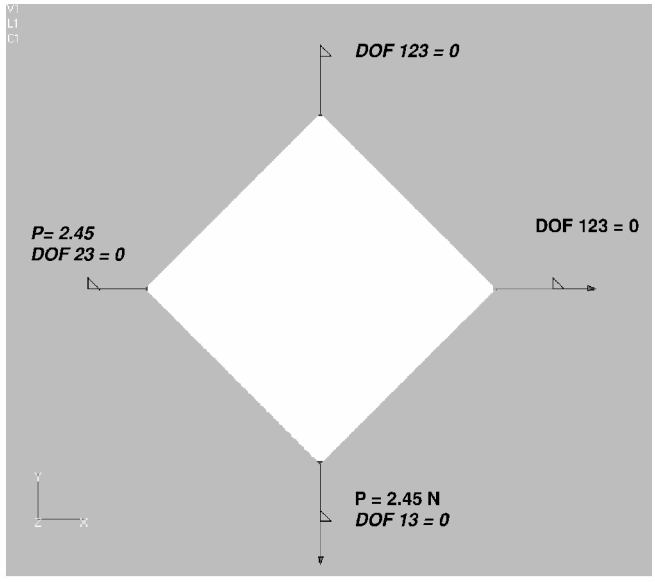

Fig. 9 Finite element model of membrane experiment.

Analytical Results

The structural response of the membrane was analyzed for each of the four load cases investigated in the laboratory experiments. Table 4 presents a summary of the maximum stress and the stress at the center of the membrane for each of the load cases. The stress levels are consistent with those of future gossamer spacecraft applications such as the NGST sunshield.[4] Plots of the major and minor principal stress distributions in the membrane for load case 3 (2.45-N corner load) are given in Figs. 10a and 10b. Figure 10a (major principal stresses) shows that there are stress concentrations at the corners of the membrane where the loads are applied; however, the central region of the membrane has a relatively uniform stress distribution. Figure 10b (minor principal stress) reveals that there is a region of near-zero minor principal stress around the corners and outside edges of the membrane. Recall from Stein–Hedgepeth theory[1] that the minor principal stresses are zero in wrinkled regions of the membrane. Figure 10c presents a plot of the predicted wrinkled region in the membrane for load case 3 (2.45-N corner load). Figures 10a–10c were generated by outputting the element integration point states during the course of the analysis. The wrinkled region is seen to extend from the corners around the edges of the membrane. Note that a comparison of the size and shape of the wrinkled region for each of the four load cases shows that the magnitude of the corner loads has an insignificant effect on the characteristics (shape and size) of the wrinkled region.

Comparison of Analysis and Experiment

Predictions from the finite element analysis were compared with results from the laboratory experiments. Because the analysis technique is not capable of predicting the details of the membrane

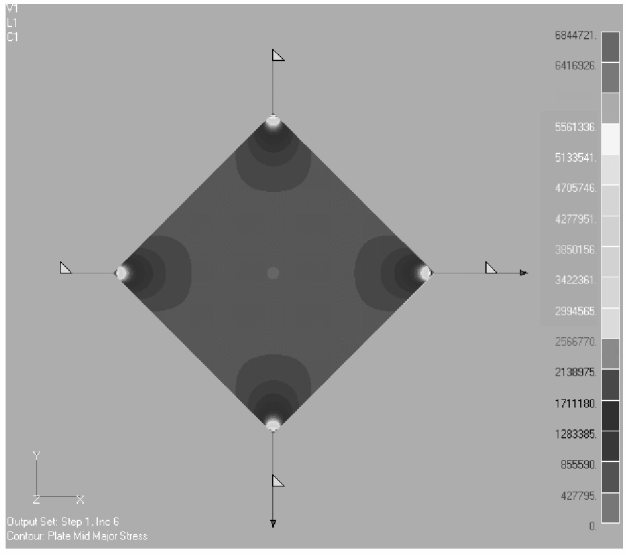

a) Major principal stresses

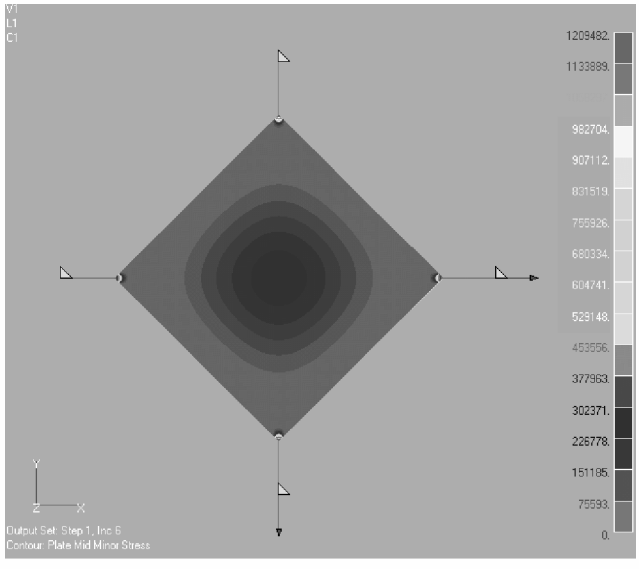

b) Minor principal stresses

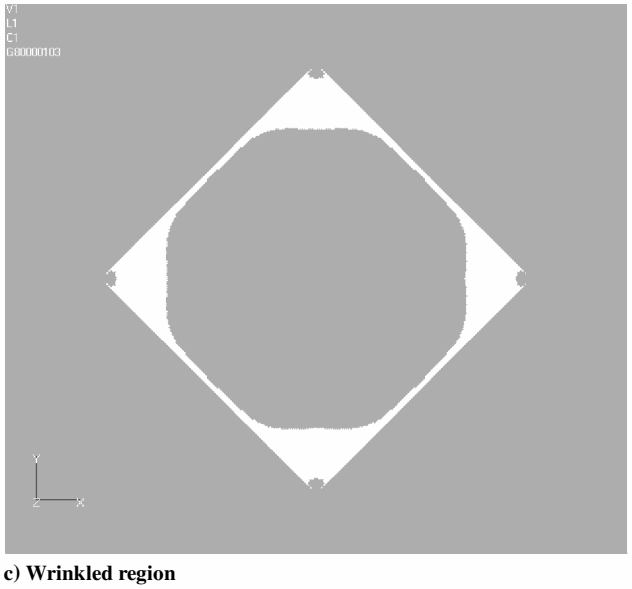

c) Wrinkled region

Fig. 10 Finite element analysis predictions for the case 3 (2.45-N corner load).

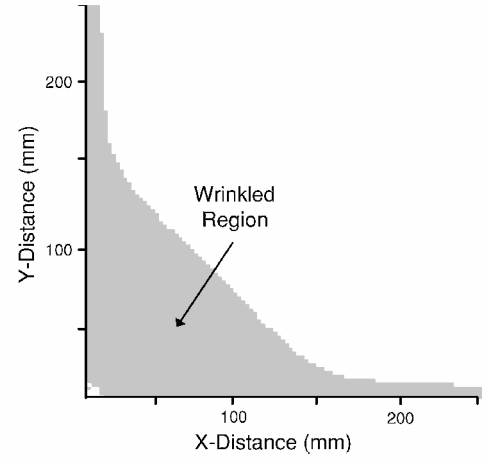

a) Predicted wrinkled region

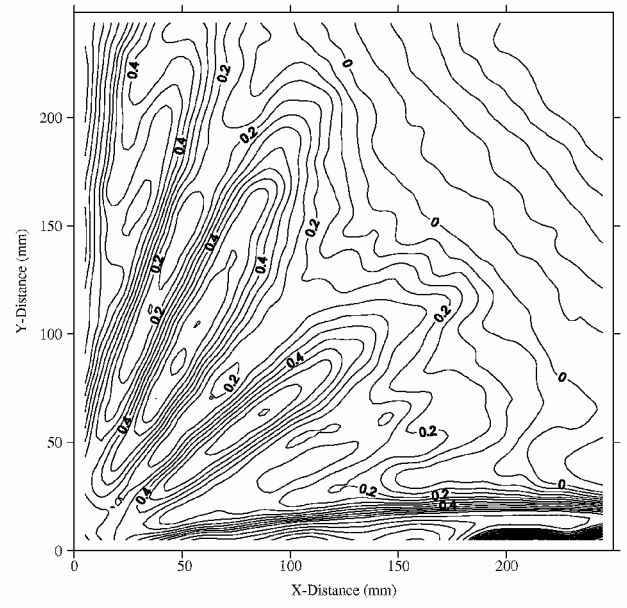

b) Measured wrinkled region

Fig. 11 Comparison of predicted and measured wrinkle regions in right-hand corner of membrane for a 2.45-N corner load.

wrinkling, comparisons are made for the extent of the wrinkled region and the direction of the wrinkles. Figure 11 provides a comparison of the predicted and measured wrinkled regions. The general shape of the wrinkle zone is seen to be similar, although the analysis predicts a smaller wrinkled region than is measured in the laboratory. The extent of the predicted wrinkled region extends approximately 43% of the distance from the corner to the center of the membrane, whereas the measured region extends approximately 59% of this distance. The comparison is somewhat complicated in that there is not a well-defined boundary to the wrinkle zone in the experimental data. Adler et al.[3] observed that a similar test geometry also showed a larger wrinkled region near the corners than was predicted by analysis.

Figure 12 presents a comparison of the predicted major principal stress directions and the measured wrinkle angles (for both the valleys and peaks of the wrinkles) in the left-hand corner of the membrane. Both angular measurements are taken from the X axis as defined in Fig. 7. Recall that Stein-Hedgepeth theory[1] predicts that wrinkles form in straight lines along the direction of the major principal stresses; thus, the measured wrinkle angles are expected to fall along the predicted major principal stress angles. Good agreement between the predicted and measured results is seen in the central region, whereas the results show less favorable agreement toward the edges of the membrane. The less favorable agreement near the

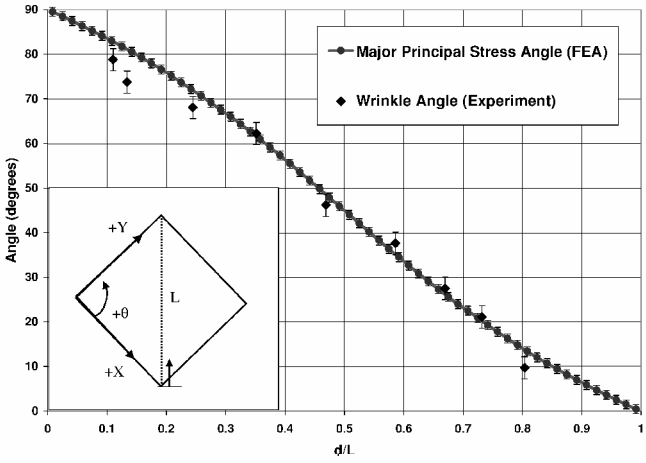

Fig. 12 Comparison of predicted major principal stress directions and measured wrinkle angles in left-hand corner of membrane; note that *d/L* is the fraction of the distance along the line joining *X* = 150 mm to *Y* = 150 mm.

edges is explained to a certain degree by the less well-defined nature of the wrinkles near the edges of the membrane in the experimental data.

Conclusions

A combined experimental and computational investigation of corner wrinkling of a square Kapton membrane was presented. The membrane was subjected to symmetric corner loads that ranged from 0.49 to 4.90 N. The wrinkling behavior of the membrane was characterized in the laboratory using photogrammetry. The experimental results showed that as the loads increased the number of wrinkles increased, but the amplitude decreased. An analysis of the experiments was performed using a computational technique that accounts for membrane wrinkling effects. Relevant results from the analytical model include predictions for the extent of the wrinkled region and the directions of the wrinkles. The experiments showed that the wrinkled region was somewhat larger than that predicted by the model. Theory predicts that wrinkles will form along straight lines in the direction of the major principle stresses. The computational results show reasonably good agreement between the measured wrinkle angles and the predicted major principal stress directions.

References

[1]Stein, M., and Hedgepeth, J. M., "Analysis of Partly Wrinkled Membranes," NASA TN D-813, 1961.

[2]Jenkins, C. H., and Leonard, J. W., "Nonlinear Dynamic Response of Membranes: State of the Art," *Applied Mechanics Reviews*, Vol. 44, No. 7, 1991, pp. 319–328.

[3]Adler, A. L., Mikulas, M. M., and Hedgepeth, J. M., "Static and Dynamic Analysis of Partially Wrinkled Membrane Structures," AIAA Paper 2000-1810, April 2000.

[4]Lienard, S. L., "Characterization of Large Thin Film Membrane Dynamic Behavior with UAI-NASTRAN Finite Element Solver," Society of Automotive Engineers, SAE Paper 199-01-5518, Oct. 1999.

[5]Johnston, J., and Lienard, S., "Modeling and Analysis of Structural Dynamics for a 1/10th Scale Model NGST Sunshield," AIAA Paper 2001-1407, April 2001.

[6]Xinxiang, L., Jenkins, C., and Schur, W., "Fine Scale Analysis of Wrinkled Membranes," *Journal of Computational Engineering and Science*, Vol. 1, No. 2, 2000, pp. 281–298.

[7]Wong, Y. W., "Analysis of Wrinkle Patterns in Prestressed Membrane Structures," M.S. Thesis, Dept. of Engineering, Univ. of Cambridge, Cambridge, England, U.K., Aug. 2000.

[8]Sewall, J. L., Miserentino, R., and Pappa, R. S., "Vibration Studies of a Lightweight Three-Sided Membrane Suitable for Space Application," NASA TP-2095, Jan. 1983.

[9]Thomas, M., and Veal, G., "Highly Accurate Inflatable Reflectors," U.S. Air Force Rocket Propulsion Lab., AFRPL Rept. TR-84-021, 1984.

[10]Jenkins, C. H., Haugen, F., and Spicher, W. H., "Experimental Measurement of Wrinkling in Membranes Undergoing Planar Deformation," *Experimental Mechanics*, Vol. 38, No. 2, 1998, pp. 147–152.

[11]Kukathasan, S., "Vibration of Prestressed Membrane Structures," M.S. Thesis, Dept. of Engineering, Univ. of Cambridge, Cambridge, England, U.K., Aug. 2000.

[12]Pappa, R. S., Giersch, L. R., and Quagliaroli, J. M., "Photogrammetry of a 5m Inflatable Space Antenna with Consumer Digital Cameras," NASA TM-2000-210627, Dec. 2000.

[13]Blandino, J. R., Johnston, J. D., Miles, J. J., and Soplop, J. S., "Thin Film Membrane Wrinkling due to Mechanical and Thermal Loads," AIAA Paper 2001-1345, April 2001.

[14]"ABAQUS/Standard User's Manual," Ver. 6.1, Hibbitt, Karlsson, and Sorensen, Inc., Pawtucket, RI, 2000.

[15]Adler, A. L., "Finite Element Approaches for Static and Dynamic Analysis of Partially Wrinkled Membrane Structures," Ph.D. Dissertation, Dept. of Aerospace Engineering, Univ. of Colorado, Boulder, CO, 2000.

[16]Miller, R. K., and Hedgepeth, J. M., "Algorithm for Finite Element Analysis of Partly Wrinkled Membrane Structures," *AIAA Journal*, Vol. 20, No. 12, 1982, pp. 1761–1763.

[17]Kang, S., and Im, S., "Finite Element Analysis of Wrinkling Membranes," *Journal of Applied Mechanics*, Vol. 64, June 1997, pp. 263–269.

C. Jenkins
Guest Editor